GOLD

Growing energy crops on contaminated land for biofuels and soil remediation

D1.1

Site description and characterization

This project has received funding from the European Union's Horizon 2020 Research and Innovation Programme under Grant Agreement No. 101006873.

Document Summary

Deliverable Number: 1.1

Version: Final

Due date: 28.02.2022

Actual submission date: 07.06.2022

Work Package 1– Title: Optimization of lignocellulosic energy crops for phytoremediation purposes

Task 1.1. – Title: Site characterization and description

Lead beneficiary: AUA

Editors/Authors: PAPAZOGLOU Eleni G., KOTOULA Danai, KAPERDAS Nick, ALEXOPOULOU Efthymia, IORDANOGLOU Konstantinos, TSIPAS George, WOJCIK Gosia, VANGRONSVELD Jaco, OUSTRIERE Nadège, OFORI-AGYEMANG Félix, KHOMSKA Olena, FIKRI ALVIN Eldo, ROY Venance, MENCH Michel, WATERLOT Christophe, ZEGADA-LIZARAZU Walter, PERONI Pietro, MONTI Andrea, WANG Yufu, ZHAO Xinlin, IQBAL Yasir.

Dissemination level: Public

1. Document history

Version	Date	Beneficiary	Author/Reviewer
1.1	07-06-2022	AUA	Eleni G. Papazoglou

Horizon 2020 Grant Agreement Number: 101006873

Project Start Date: 1 May 2021

Duration: 48 months

Project coordinator: CRES

Partners

CRES - Centre for Renewable Energy Sources and Saving Foundation, Greece
AUA – Geoponiko Panepistimion Athinon, Greece
TUM - Technische Universität München, Germany
RE-CORD - Consorzio per la Ricerca e la Dimostrazione sulle Energie Rinnovabili, Italy
ETA - ETA Energia, Trasporti, Agricoltura, Italy
Uni-Lublin - Uniwersytet Marii Curie-Sklodowskiej, Poland
TNO - Nederlandse Organisatie Voor Toegepast Natuurwetenschappelijkonderzoek TNO, Netherlands
CERTH - ETHNIKO KENTRO EREVNAS KAI TECHNOLOGIKIS ANAPTYXIS, Greece
UNIBO - Alma Mater Studiorum - Università di Bologna, Italy
INRAE - Institut National de Recherche pour l'Agriculture, l'Alimentation et l'Environnement, France
YNCREA HDF – Junia, France
UNL - Universidade Nova de Lisboa, Portugal
ICL - Imperial College of Science Technology and Medicine, United Kingdom
WR - Stichting Wageningen Research, Netherlands
METE S.A. - METE AE METALLEFTIKI EMPORIKI TEHNIKI AE*MINING TRADING TECHNICAL SA, Greece
IITD - Indian Institute of Technology Delhi, India
HUNAN - Hunan Agricultural University, China
UDES - Université de Sherbrooke, Canada
IBFC - Institute of Bast Fiber Crops, Chinese Academy of Agricultural Sciences, China

Executive Summary

Soil pollution due to global anthropogenic and geogenic activities is a worldwide concern and the number of contaminated sites is increasing year by year. It has been estimated that in Europe a total area covering roughly 650,000 ha could be defined as contaminated with organic and/or inorganic pollutants, and almost 60% relates to mineral oil and/or heavy metals and metalloids. One of the objectives of GOLD project is to exploit contaminated lands by cultivating selected high-yielding lignocellulosic energy crops, and, in long-term, to return these lands back to the agricultural production. Seven experimental fields have been selected in Greece (two), Italy, France, Poland, and China (two) covering different agro-ecological zones. An inventory of climatic data, of soil physico-chemical characteristics, and of the levels and type of contaminants of the experimental sites have been accomplished. The results showed that the most frequently found element is Cd, determined in the fields of AUA, UMCS, YNCREA, IBFC, HUNAU. Next are the elements: Pb and Zn (AUA, UMCS, UNIBO, YNCREA); Ni (AUA, CRES, UNIBO); AS (AUA, CRES, UMCS); Cu (UNIBO, YNCREA). In one site the elements Cr (CRES), Sn (UNIBO), Co (CRES), Sb (AUA) are found. These sites poses risks for human health if they are used for food production or grazing and are in need for remediation. Therefore, developing, presenting and promoting the GOLD green technology is an important step of improvement, and will be a valuable guide to mitigate the exposure route for the intake of contaminants by humans.

Table of contents

2. List of figures

I. Introduction

Soil pollution is a global problem occurring where intensive industrial activities, inadequate waste disposal, mining, extensive use of agrochemicals (pesticides and fertilizers), combustion of fossil fuels, etc. introduced excessive amounts of organic and/or inorganic pollutants into the soil. It has been estimated that in Europe there are 2.5 million of potentially contaminated sites, of which about 14% (340,000 sit es) are expected to be contaminated and require remediation (Van Liedekerke et al., 2014; Mench et al., 2018). A total area covering roughly 650,000 ha could be defined as contaminated with organic and/or inorganic pollutants (Paya Perez et al., 2018), and almost 60% relates to mineral oil and/or heavy metals and metalloids (HM&M) (Panagos et al., 2013).

In GOLD project and under the frame of WP1, small scale field trials will be established in contaminated sites of two continents (Figure 1.1). In Europe, the sites were selected so as to represent the main agro-climatic zones and farming systems, namely: a) Mediterranean North and South (UNIBO-IT, AUA-GR and CRES-GR) that has short precipitation periods, hot and dry summers, and air temperatures favourable for growing a wide range of crops, b) Continental (UMCS-PL) that covers most part of Europe and is characterized by high temperatures in summer and very low in winter, followed by relatively high precipitation and c) Atlantic (YNCREA-FR) that generally features cool summers (relative to their latitude) and cool but not cold winters, a more temperate climate through the year with high precipitation levels. In Asia, field trials will be established in: a) two sites in Hunan province in China (HUNAU-CN, IBFC-CN), having humid subtropical climate (Cfa per Köppen-Geiger classification), warm and temperate climate with a significant amount of rainfall during the year and b) one site in India (IIDT-IN) having Monsoon-influenced humid subtropical climate (Cwa per Köppen-Geiger classification).

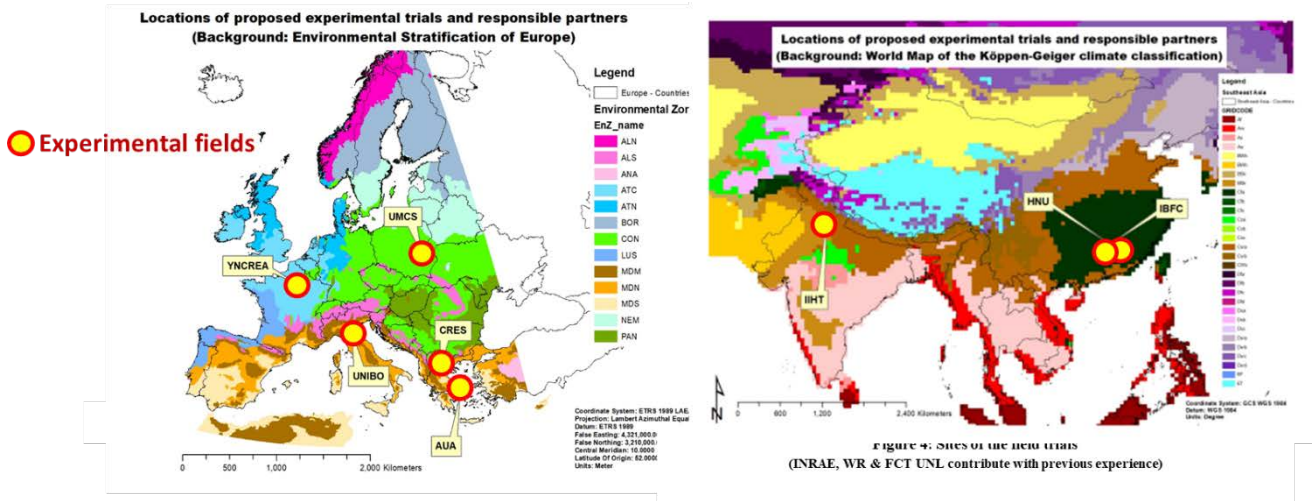

Figure 1. Locations of WP1 field trials In Europe and Asia and partners involved.

In the present deliverable an inventory of the soil physico-chemical characteristics and of the level and type of contaminants of the experimental sites is presented. In addition, the climatic data per site is included.

II. Site characterization and description

The selected sites are unused and/or abandoned arable lands suitable for mechanized agricultural crop production. The soil physico-chemical characteristics are determined following standard procedures. The total concentrations of the heavy metals and metalloids were analyzed after soil sample digestion with *aqua regia* ($HCl:HNO_3$, 3:1 v/v). It is also important to know the potential bioavailability of HM&M in soil; however, only a fraction of the trace elements that is bioavailable at a specific moment and for an organism in question can be estimated, since the bioavailability is a dynamic process that varies in time and space (Kumpiene et al., 2017). The partners involved in WP1 decided to evaluate the HM&M potential bioavailability using the mild extractants $CaCl_2$ or $Ca(NO_3)_2$. The characterization and description of the selected sites is presented separately per partner and country in the next sections.

1. AUA, GREECE

1.1. Site presentation

The experimental field of GOLD project is located in Thorikon of Lavreotiki peninsula (SE of Attica, 37°43'59''N, 24°02'40''E, 5 m a.s.l.), in a distance of 3 km from the city of Lavrion (Figure 1.1). This area is long-term contaminated, mined for lead and silver ores (mainly galena - PbS) since the late Neolithic era (4200–3100 BC) (Kakavoyianni et al., 2008). These activities were strongly intensified from the late Archaic period (540–480 BC) onwards (Kakavoyiannis, 2005). During the late Classical (400–323 BC) and Early Hellenistic period (323–250 BC) the area was gradually built up with ore processing workshops. As a result, the area was transformed into a state-run industry, which had a huge impact on the environment. The waste materials generated by ancient Greeks, after exploitation of the richest ores, were: (i) the mine tailings, (ii) washing plant debris or flotation tailings, (iii) slag, and (iv) litharge (Tristan et al., 1999).

Figure 1.1. GOLD experimental field in Lavreotiki peninsula, Attika, Greece.

More recent (1864-1982 A.D.) mining and smelting activities resulted in an additional burden of soils with toxic elements. It is estimated that -from ancient to recent times- the total tonnage of lead produced from the exploitation of ore from the area is 2260000 tonnes and of silver 4500 tonnes. The corresponding excavating material is approx. 4300000 tonnes, exposed to the processes of erosion and deposition (Tristan et al., 1999). It is obvious that the area is a toxic hotspot and the local population is exposed to multiple hazardous pollution sources. Epidemiological studies conducted in the wider urban area of Lavrion city revealed that, for 95% of children, Pb levels in blood exceed the tolerable limit of 100 mg L^{-1} suggested by the World Health Organization

(Xenidis et al., 2003). Indicative total concentrations of heavy metals and metalloids in the wider area (mg kg^{-1}) are shown in Table 1.1.

Table 1.1. Heavy metal and metalloid total concentrations (mg kg^{-1}) in the soil of the wider area of Lavreotiki peninsula.

	As	Cd	Co	Cr	Cu	Fe	Mn	Ni	Pb	Sb	Zn
mg kg^{-1}	3430.7	132.5	7.6	127.4	724.9	40042.5	2948.2	146.8	32699.8	369.6	20217.3

1.2. Soil physico-chemical properties and contamination

Seven surface soil samples (depth 0-20 cm) were collected from the experimental field (Figure 1.2), and selected soil characteristics were determined following standard procedures (Table 1.2).

Figure 1.2. Sampling points of GOLD experimental field in Lavreotiki peninsula, Attika, Greece.

The soil texture was clay-loam (CL) apart from the sampling points 1 and 6 in which the soil texture was loam (L) and sandy clay loam (SCL) respectively. The pH ranged between 7.8 and 8.2 indicating that the soil is slightly to moderate alkaline. The organic matter content ranged between 1.57 g kg^{-1} (low) to 3.73 g kg^{-1} (normal) while the cation exchange capacity was normal (12.8-22.2 meq Na $100g^{-1}$). The equivalent CaCO3 was rich (11.76-15.54 g $100g^{-1}$) and the total nitrogen ranged between low (point 6) and high (point 7). In all other sampling points the total nitrogen was slightly low. The exchangeable K_2O was rich and this has to be taken under consideration in the fertilization management of the field. Available Cu was high with an average 10.4 g kg^{-1} and the water soluble B ranged between normal (0.83 g kg^{-1}) and high (1.22 g kg^{-1}). Available P_2O_5 was generally low in all sampling points, apart from point 3 where it was up to 16.9 g kg^{-1}, indicating that phosphorus should be added to the soil.

The elemental analysis showed an extremely high soil pollution of the experimental field. The total concentrations where much higher than the normal values defined by Kabata-Pendias, 2000 and Kabata-Pendias and Mukherjee, 2007. Lead and zinc ranged between 3588 and 8707 mg kg^{-1} and 2789 and 6137 mg kg^{-1} respectively. Giving the fact that normal values for both heavy metals in soils are defined as up to 300 mg kg^{-1}, their concentrations were 12-728 and 3.8-1602 fords higher than normal. Nickel concentrations were 156-201 mg kg^{-1}, namely 2.1 to 2.7 folds higher than the normal value of up to 75 mg kg^{-1}. Cadmium concentrations ranged between 6.3 and 21.8 mg kg^{-1}, namely 2.5 and 8.6 folds higher than normal (up to 2.5 mg kg^{-1}). The metalloids arsenic and antimony were also measured in increased concentrations, i.e. 165-691 mg of As per kg of soil and 6.8-120 mg of Sb per kg of soil. The corresponding normal values were up to 2.5 and 1 mg kg^{-1} respectively. Both metalloids were 66-276 folds for As and 6.8-120 folds for Sb higher than normal values.

Table 1.2. Soil physico-chemical characteristics of the experimental field.

Parameters	Units	Range
Clay	g $100g^{-1}$	22-35
Silt		25-34
Sand		31-53
pH		7.8-8.2
Organic matter	g kg^{-1}	1.57-3.73
CEC	meq Na $100g^{-1}$	12.8-22.2
EC	µS cm^{-1}	109-264
Equivalent CaCO3	g $100g^{-1}$	11.76-15.54
Total Nitrogen	g kg^{-1}	0.10-0.22
Exchangeable K_2O	g kg^{-1}	304-845
Available Cu		6.4-15.1
Water soluble B		0.83-1.22
Available P_2O_5 (Olsen)		7.5-16.9

The $CaCl_2$ extractable concentrations were much lower than the total. However, Cd, As and Sb concentrations were measured to be higher than the normal values (Table 1.3). In addition Cd was the highest extractable metal, followed by Ni>As>Zn>Sb>Pb.

In conclusion, the soil of the experimental field is highly contaminated. However, due to increased pH and the soil texture (CL) the bioavailable concentrations are low and only Cd, As and Sb exceed the normal values posing risks to human health if the site is used for food production.

Table 1.3. Heavy metal and metalloid concentration in soil. Values in red are above the normal values defined by Kabata-Pendias, 2000 and Kabata-Pendias and Mukherjee, 2007.

	Pb	Zn	Ni	Cd	As	Sb
			Total concentrations (mg kg^{-1})			
Range	3588-8707	2789-6137	156-201	6.3-21.8	165-691	6.8-120
Mean	5835.7	4790.7	186.6	17.1	516.4	59.8
SD	1033.3	987.1	15.3	2.7	141.2	21.5
			Calcium chloride extractable concentrations (mg kg^{-1})			
Range	30.6-106.1	92.2-231.5	4.9-23.3	1.6-6.6	9.9-53.4	0.2-1.9
Mean	65.2	171.9	15.7	5.8	40.3	1.0
SD	17.7	43,7	4.4	1.5	9.1	0.2

1.3. Climatic data

The study site belongs to the Mediterranean Agro-ecological zone, characterized by mild, wet winters and hot, dry summers. The coldest period is from October until April, while the warmest is from May until September. The max and min temperatures observed are usually around 31°C (July and August) and 9 °C (January) respectively (Figure 1.4). The average annual rainfall is below 200 mm (Figure 1.5), with the highest precipitation in December and the lowest (or even no rainfall at all) in July and August. Another characteristic of the area is the prevailing north wind, with an average speed of 13 to 22 km h^{-1}. The highest relative humidity is in winter months (November-February) and range between 70 and 77 % while the lowest is in July and August (45-53%).

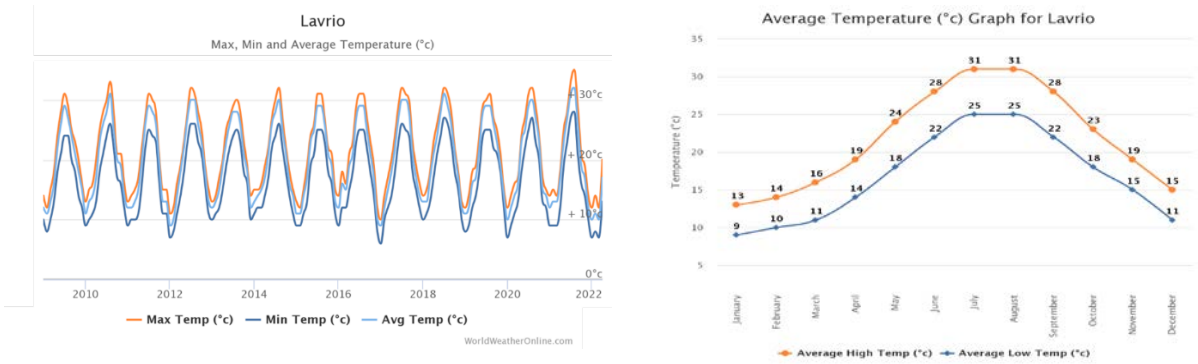

Figure 1.4. Maximum, minimum and average temperatures (°C) for the period 2009-2021, and monthly high and low temperatures (°C) in the study site.

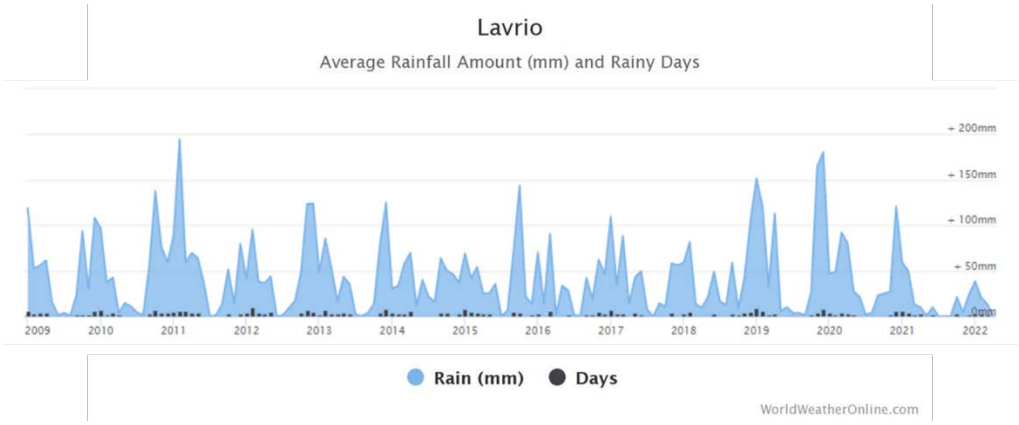

Figure 1.5. Average rainfall (mm) and rainy days in the study site.

2. CRES, GREECE

2.1. Site presentation

The second experimental field of GOLD project in Greece is situated in the Region of Western Macedonia, Prefecture of Kozani, in the location Prosilio of the municipality of Serbia – Velvento. The field belongs to the private company METE S.A., which mines lignite from the ore deposits in an area of 2.7 km^2 (Figure 2.1).

During the excavation activities, the sterile mining materials are deposited in the gaps created by the excavations and, thereinafter, METE restore the site by planting and seeding (Figure 2.2).

Figure 2.1. Experimental plot in Servia (Google Earth, 2022).

One of the major existing problems are the disturbances of the agricultural life-activities, due to the high concentrations of Ni, Zn, and Cu, noting that Ni, Zn and Cu were found doubled, tripled or even more higher than normal concentrations (Papadopoulos et al. 2007). In these fields, food crop cultivations are not allowed and cannot be sustained due to the high metal(loid)s concentration, as a result the cultivation of non-food is necessitate.

The experimental plot of 0.5 ha, mainly contaminated by Ni, Zn, Cr and Cu, is located in Servia, near Kozani city (Figure 2.3). The experimental plot is an inclined contaminated area, inhabited by wild herbaceous or non-herbaceous species including trees. Noting that this site has data and applications available from past years, concerning agricultural activities (such as pastures), sowing with *Lolium perenne* and other species, mainly Faboideae *taxa*, by the METE company, when reclaiming the area that the lignite extraction took place.

Figure 2.2. Lignite mine PROSILIO in the year 1997 (left) and in the year 2019 (right) (https://www.mete.gr).

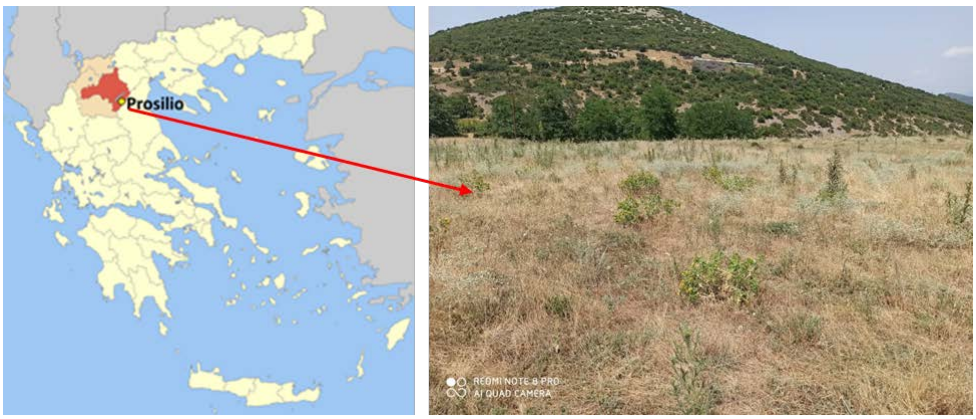

Figure 2.3. Location of GOLD site in Kozani/Greece and photo of the experimental field.

2.2. Soil physico-chemical properties and contamination

Soil samples were taken from 5 points of the experimental field and were analysed for their physico-chemical characteristics and trace element contamination (Table 2.1). The pH values ranged between 7.8 and 8, characterizing the soil as slightly alkaline, an expected value due to the demineralization of the experimental area mainly from the rainfalls and other natural factors (such as bacteria, other plants, fungi). The average metal concentrations are: Pb=7.4 mg kg^{-1}, Zn=29.0 mg kg^{-1}, Ni=729.0 mg kg^{-1}, Cd<bdl, Cu=12.4 mg kg^{-1}, Cr=167.8 mg kg^{-1}, Co=42.4 mg kg^{-1}, As=4.5 mg kg^{-1}, and Sb<bdl. Most of the calcium chloride exctractable fractions were below detection limit, apart from nickel (Table 2.1).

Table 2.1. Soil contamination with heavy metals and metalloids. Values marked in red are above the normal values defined by Kabata-Pendias, 2000 and Kabata-Pendias and Mukherjee, 2007.

	Pb	Zn	Ni	Cd	Cu	Cr	Co	As	Sb
Total concentrations (mg kg^{-1})									
Range	3-12	20.2-38.0	58.5-1256.4	bdl	8.9-15.6	22.9-412.4	7.1-69.9	1.7-6.2	bdl
Mean	7.4	29.7	729.1	-	12.4	167.8	42.4	4.5	-
SD	2.9	6.3	285.9	-	1.9	64.5	11.1	1.2	-
Calcium chloride extractable concentrations (mg kg^{-1})									
Range	bdl	bdl	bdl-386.7	bdl	bdl	bdl-36.8	bdl	bdl	bdl
Mean	-	-	105.6	-	-	11.8	-	-	-
SD			87.3			7.7			

bdl: below detection limit

2.3. Climatic data.

Monthly climatic data were acquired from the meteorological station located at Velvento, Kozani approximately 30 kilometres North East of the field, in order to calculate average temperature, rainfall and wind velocity, in the area. Also, data about relative humidity were acquired from the meteorological station of Adrassa, due to the fact that Velvento station did not recorded these data. The climatic data cover the chronological period of 5 years (2016 until 2020).

The region of Servia, Kozani benefits from a continental climate with cold winters and hot, rainy summers (Figure 2.4). Average temperature through the last five years was around 15.5°C. Although, from November until February the minimum temperature seems to drop below -10°C, due to the relatively high elevation level of the area, about 550m above sea-level and the mountainous terrain. Minimum temperature seems to drop below 0°C almost every December and January, on the other hand, the temperature can reach 40°C during June and July every year. There is no significant differences between the years, which are showing that the main target is to protect plants during December and January and to provide higher irrigation doses in June and July due to higher evapotranspiration rate.

Sum of yearly precipitation measured in mm for 5-year period and an ombrothermal diagram are shown in Figure 2.4. Precipitation during summer months of the last five years seems to be quite high with the lowest average value be 27mm in the summer of 2016 and highest average value be 132.4mm in 2020. To conclude with, precipitation seems to be able to cover the cultivar's needs for water, when temperatures are high. Although irrigation is recommended, because the precipitation in June and July is high, but it is not equally distributed throughout the month.

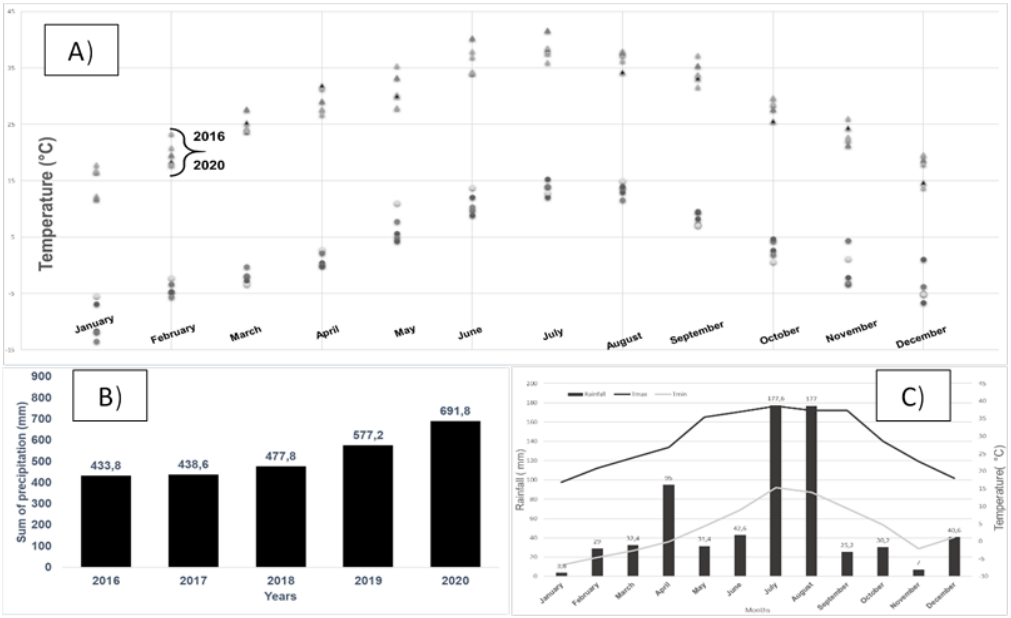

Figure 2.4. A) Maximum and minimum monthly temperatures during a 5-year period. B) Total precipitation through 5 years at Velveto Kozanis. C) Ombrothermal diagram at Velveto in 2020.

Average relative humidity over the past five years is presented in Figure 2.5. Through the last five years the highest relative humidity recorded at February of 2018 of 81.25%, while the minimum recorded at August of 2019 with 56.1%. The average humidity seems to achieve high peaks in the months between November and February, although during spring relative humidity doesn't seem to drop below 60%. August and December are the months averaging with the lowest relative humidity. As for the year 2020, relative humidity seems to average less than the other years with June and September recording lowest values at 61.05% and 60.4%, respectively, while the higher values recorded in March and December (Figure 2.5.B) at 70.65% and 78.25%, respectively.

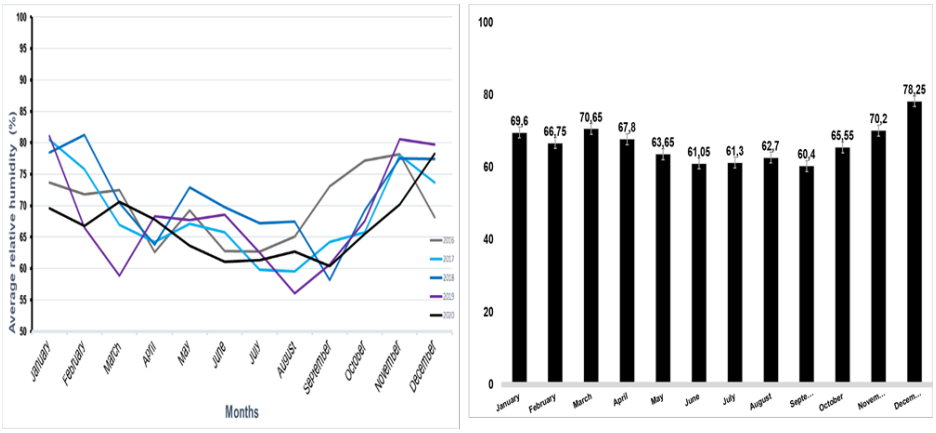

Figure 2.5. A) Monthly changes of relative humidity at Velento during a 5 year period (2016-2020). B) Monthly changes of relative humidity during 2020.

Wind data in Figure 2.6 are indicated that throughout the last five years, wind speed does not grow higher than 30 Km/h and that highest wind velocity usually occur between February and March or during July. Thus, the low velocity of wind in the area can be beneficial in order to avoid the danger of lodging. As for direction, the SE wind direction seems to be the dominant.

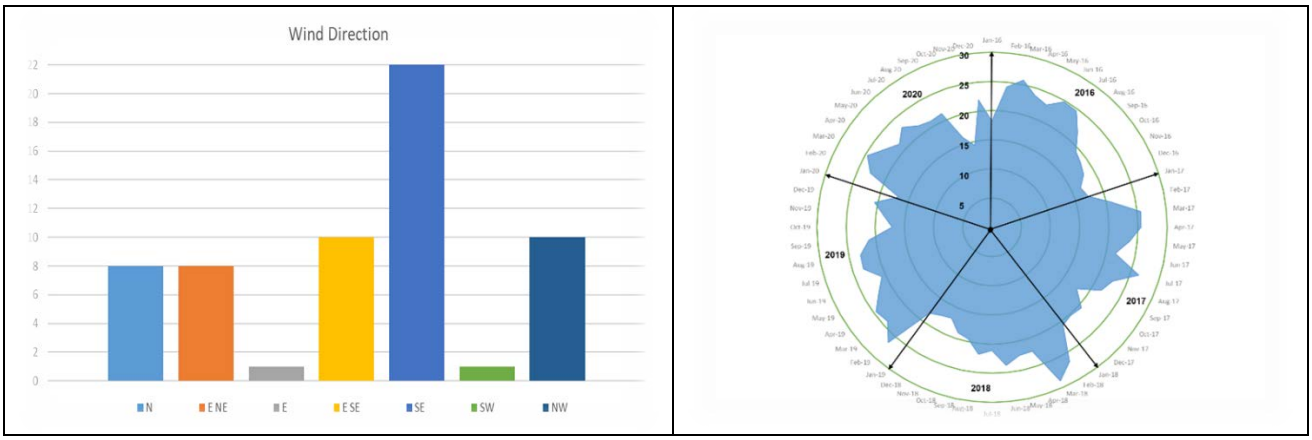

Figure 2.6. A) Number of monthly wind direction data 2016-2020 B) Monthly air velocity 2016-2020.

3. UMCS, POLAND

3.1. Site presentation

The study area is located in the administrative region of the city of Piekary Śląskie – the residential district Dołki, in the Upper Silesia Industrial Region, southern Poland (50°21'19" N; 19°00'17" E) (Figure 3.1).

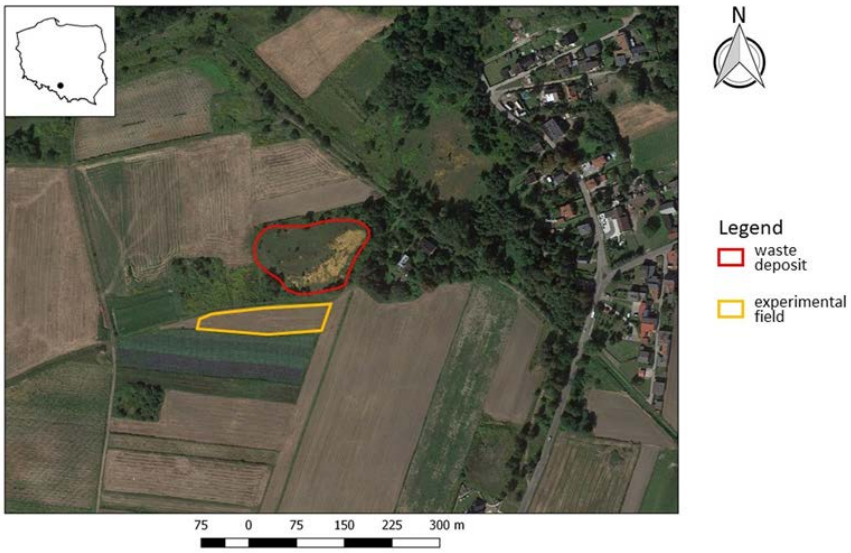

Figure 3.1. The location of the experimental field.

An experimental field, of appr. 0.25 ha area, is partially neighbouring from the north with an old metalliferous waste dump, which is the main source of the metallic pollution to the surrounding areas (Figure 3.1). The waste dump was created during the period from the end of the 19th century until the years 1915-1930 and deposited the wastes from the gravitational enrichment of Zn-Pb ore – zinc blende by mining and metallurgy plant "Orzeł Biały"(formely "Blei Scharley"). The waste heap occupies an area of more than 1.2 hectares and its altitude is over 11 m. The metal content of the waste heap substrate is high, comprising up to ca. 17% Zn, ca. 2.2% Pb and ca. 0.1% Cd, at slightly alkaline reaction of the top soil (Kucharski et al. 2010; Wójcik et al. 2014).

In the immediate vicinity of the dump there are residential buildings, allotment gardens and fields planted with grain and vegetable plants (Figure 3.2).

Figure 3.2. Photographs showing the experimental field (yellow arrows) visible from the top of the waste deposit (upper two photographs) or from other directions (lower two photographs)

3.2. Soil physico-chemical properties and contamination

Six composite soil samples of 0-20 cm depth were collected and analysed. Based on the cumulative data of soil separates, the soil exhibited a silty loam texture (i.e. 31.5% sand, 60.1% silt, 8.4% clay), according to the United States Department of Agriculture (USDA) soil texture classification. The soil samples were neutral to slightly alkaline, with a pHH2O range from 7.37 to 7.6 (pHKCl range from 6.59 to 6.75). The total nitrogen content ranged from 0.15 to 0.23%, with a mean of 0.17%. The total carbon content averaged at 3.2% (2.35-4.74%), of which organic carbon comprised 2.31-3.26%. The available phosphorus and potassium contents were high to very high, in ranges 5.81-18.38 (mg P_2O_5 100 g^{-1}) and 11.64-46.48 (mg K_2O 100 g^{-1}), averaging 9.73 mg 100 g^{-1} for P_2O_5 and 24.43 mg 100 g^{-1} for K_2O. The values of hydrolytic acidities (Hh 1.46-1.66) were low in comparison to TEB (9.1-18.83) resulting in the very high saturation of the sorption complex with exchangeable bases (86.15-92.26%).

The elemental analysis indicated a significant soil pollution with trace elements. The total concentrations of the metals Zn, Pb, and Cd and the metalloid As in the soil samples exceeded their respective permissible limits for

soils used for agriculture established by Polish Ministry of Environment (2002) (300, 100, 4, and 20 mg kg^{-1}, respectively) (Table 3.1). Zinc concentrations ranged from 6110.9 to 9417.9 mg kg^{-1} (average 8057.1 mg kg^{-1}), Pb concentrations ranged from 1794.1 to 3804.5 mg kg^{-1} (average 2939.7 mg kg^{-1}), Cd concentrations ranged from 33.89 to 65.32 mg kg^{-1} (average 51.56 mg kg^{-1}), and As concentrations ranged from 72.04 to 115.0 mg kg^{-1} (average 94.13 mg kg^{-1}). The total concentrations of Cr, Cu, and Ni were in the range 18-27, 21-34.5, and 16.5-25 mg kg^{-1}, respectively, and were all much below the permissible threshold levels (established at 150 mg kg^{-1} for Cr and Cu, 100 mg kg^{-1} for Ni, Ministry of Environment, 2002).

The concentrations of extractable (by $CaCl_2$) and thus potentially available for plant uptake forms of metals were very low or below detection limits (Table 3.1). The extractable forms of Zn ranged from 1.54 to 4.17 mg kg^{-1} (average 2.856 mg kg^{-1}) which represents approximately 0.035% of the total soil Zn content. The extractable forms of Cd ranged from 0.15 to 0.305 mg kg^{-1} (average 0.195 mg kg^{-1}, about 0.387% of the total pool of Cd). The rate of extractable forms of Pb was the lowest in comparison to the total Pb content (approximately 0.011%), with their concentrations ranging from 0.22 to 0.44 mg kg^{-1} (average 0.295 mg kg^{-1}). A low contribution of potentially phytoavailable forms in the total pool of metals determined in the experimental field soil is a consequence of the relatively high pH (making metals hardly available) and results from low values of Hh and approximately 90% saturation of the sorption complex with base cations, causing strong binding of metals in the soil.

Table 3.1. Trace element concentrations in the soil samples (n=6). Values marked in red are above the permissible thresholds for agriculture soils according to Polish Ministry of Environment (2002).

	Zn	Pb	Cd	As	Cr	Cu	Ni
			Total concentration (mg kg^{-1})				
Range	6110.9 – 9417.9	1794.1 – 3804.5	33.89 – 65.32	72.04 - 115.0	18-27	21-34.5	16.5-25
Mean	8057.1	2939.7	51.56	94.13	22,05	27,37	21.14
SD	2054.2	864.1	15.0	21.9	3.7	5.0	3.2
Permissible threshold*	**300**	**100**	**4**	**20**	**150**	**150**	**100**
			Calcium chloride extractable concentration (mg kg^{-1})				
Range	1.54-4.17	0.22-0.44	0.15-0.30	nd	nd	bdl	bdl
Mean	2.856	0.295	0.195	nd	nd	bdl	bdl
SD	1.00	0.08	0.05	-	-	-	-

bdl – below detection limit, nd – not determined

3.3. Climatic data

The area where the experimental field is located belongs to the Częstochowa-Kielce agro-climatic district, lying in the transition zone between oceanic and continental climates with the dominance of air masses from the Atlantic Ocean (about 60%), high contribution of continental air masses from the east (about 30%) and only marginal influence of the Arctic and tropical air masses from the north and south, respectively. The average annual air temperature is 9°C; the warmest month of the year is July with an average temperature of 19.3°C, while the coldest month is January with an average temperature of -2.1°C.

The average annual rainfall is about 817 mm, with the highest precipitation in July (109 mm on average) and the lowest in February (36-40 mm). The lowest number of rainy days are in October (average 10.63 days) and the most in July (average 14.67 days). The time of the snow cover ranges from 60 to 90 days and the

vegetation season lasts between 200 and 210 days. The lowest relative humidity of the year is in April (67.05%). The month with the highest humidity is January (84.28%). Wind directions refer to the general atmospheric circulation and are locally modified by the terrain. Prevailing winds (for close to 10 months) are from the western directions (west, south-west and north-west) with an average speed of 3 to 4 m s-1. Due to its location in the most urbanized and industrialized parts of the Katowice conurbation, the quality of the air in the studied area is poor.

4. UNIBO, ITALY

4.1. Site presentation

The Chiarini 2 experimental site is located in the surroundings of Bologna city, Italy (44° 50' N, 11° 28' E, 36 m a.s.l.). Chiarini 2 is near the Reno River (Figure 4.1) with an unconfined water table depth of about 50-60 m, a hydraulic gradient of about 3%, and a permeability of the saturated layer between 2.10-3 to 6.10-4 m sec^{-1}. The entire area has been subject for a long time to discharge and deposition of wastes of various origins (i.e. improvised warehouses, small crafts, and processing of raw materials, industrial waste, and residues generated by World War II). The surface extension of the area actually subject to contamination is not well defined, but residues of wastes and contaminated materials have been detected up to 4 m deep. Since 2007 the entire site is fenced and capped with a HDPE film to prevent deep leaching of contaminants (i.e. heavy metals), moreover every 6 months the groundwater monitoring is carried out, but no exceeding of the legal thresholds has been recorded for any pollutant.

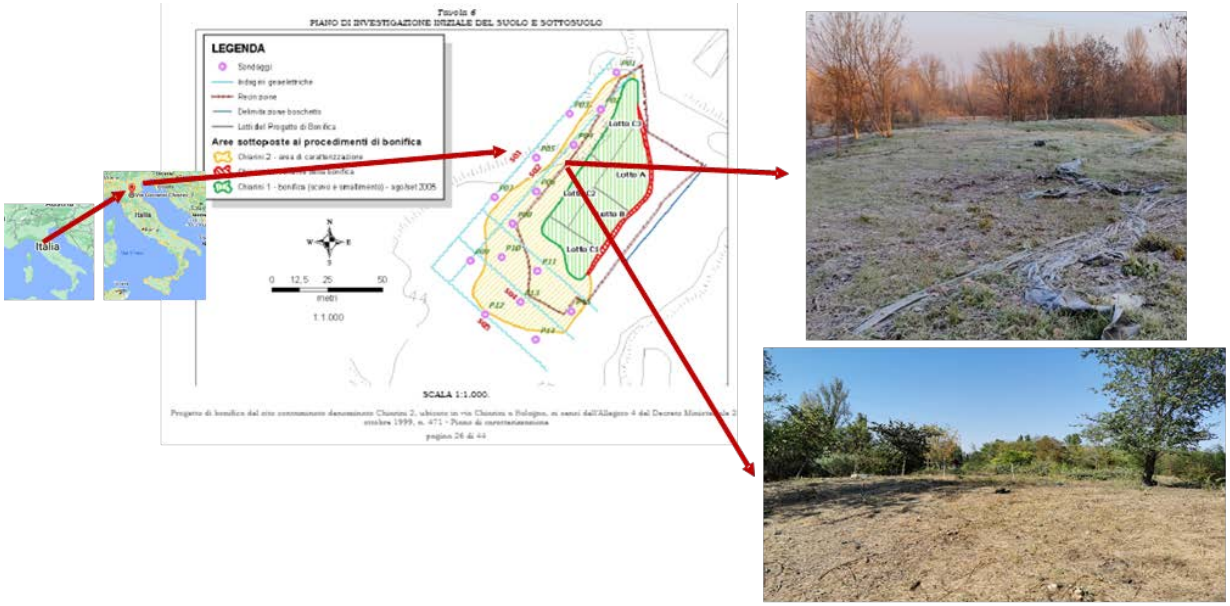

Figure 4.1. The Chiarini 2 experimental site located in the surroundings of Bologna city, Italy (44° 50' N, 11° 28' E, 36 m a.s.l.).

4.2. Soil physico-chemical properties and contamination

Soil samples were taken at 6 sampling points (S1-S5, and A) along the field to a depth of 80 cm (Figure 4.2). The analysis was carried out by a certified laboratory according to the agreed protocol within the GOLD consortium. The area has been divided in two sub-areas based on the sampling results. One to the south-west, delimited in blue in Figure 4.2, characterized by a relative uniformity in the presence of heavy metals, and one to the north-east characterized by greater variability in the concentrations of heavy metals. No pollutants have been found in the sampling point S6.

Figure 4.2. Excavation point for soil sampling and soil sampling points at the Chiarini 2 experimental site in Bologna, Italy.

The soil is sandy-loam and calcareous with medium to high active limestone (52 g kg^{-1}), low exchangeable potassium (0.8 mg kg^{-1}), low assimilable phosphorus and nitrogen contents (20 mg kg^{-1} of P_2O_5 and 0.09% of total N, respectively), moderate alkalinity (pH = 7.7), and a low organic matter content (Table 4.1).

Table 4.1. Physical and chemical characterization of the soil at the Chiarini 2 site.

Parameter	Result	U	U.M.	L.Q.
Clay	149		g kg^{-1}	0
Silt	329	± 117	g kg^{-1}	0
Sand	522		g kg^{-1}	0
pH	7.72		pH unit	4
total limestone	160		g kg^{-1}	5
active limestone	52		g kg^{-1}	5
Total organic carbon	10	± 1	g kg^{-1}	2
Organic Matter	17			
Total nitrogen	0.9		g kg^{-1}	
assimilable phosphorus	20		mg kg^{-1}	4
exchangeable potassium	0.8		meq $100g^{-1}$	
exchangeable potassium	318		mg kg^{-1}	
C/N	11.1			

Regarding heavy metals, it was detected the presence of nickel, lead, copper, zinc, and tin concentrations above the thresholds permitted by law in rural areas (Table 4.2). The analyses on the bio-available fraction of heavy

metals (extracted by calcium nitrate) showed that these fractions were below the limits of determination for all the elements assessed (Table 4.3). No significant concentrations of heavy hydrocarbons (C> 12) were detected.

Table 4.2. Total metals concentration at the Chiarini 2 site. Values marked in red are above the permissible thresholds for agriculture soils according to thresholds permitted by law in rural areas.

Parameter	Result	U	U.M.	L.Q.	Legal Threshold
Lead	159	± 32	mg kg-1 DM	1	100
Cadmium	< L.Q.			1	2
Copper	137	± 27		1	120
Nickel	209	± 42		1	120
Zinc	455	± 91		1	150
Arsenic	4.1	± 0,8		1	20
Tin	8.8	± 1,8		5	1

Table 4.3. Calcium nitrate extractable heavy metal and metalloid concentrations at the Chiarini 2 site.

Parameter	Result	U.M.	L.Q.
Lead (Pb)	*< bdl*		*0.5*
Cadmimum (Cd)	*< bdl*		*0.5*
Copper (Cu)	*< bdl*		*0.5*
Nickel (Ni)	*< bdl*	mg kg-1 DM	*0.5*
Zinc (Zn)	*< bdl*		*0.5*
Arsenic (As)	*< bdl*		*0.5*
Tin (Sn)	*< bdl*		*0.5*

bdl: below detection limit

4.3. Climatic data

The climate of the experimental site is typical of a temperate humid region with cold winters and hot summers (Figure 4.3). Normally, the plant growth season lasts from early spring (April) to the end of summer (September). Along the year, precipitations are fairly distributed, but with two well-defined peaks in spring and autumn. Summers are generally dry and hot. The long-term (2011-2020) mean temperatures from April to September are 15.3 (±4.3) and 27.3 (±4.8) °C, with an average air humidity of 61%. The average cumulated precipitation in the same period is 324 mm (about 40% of total annual precipitation).

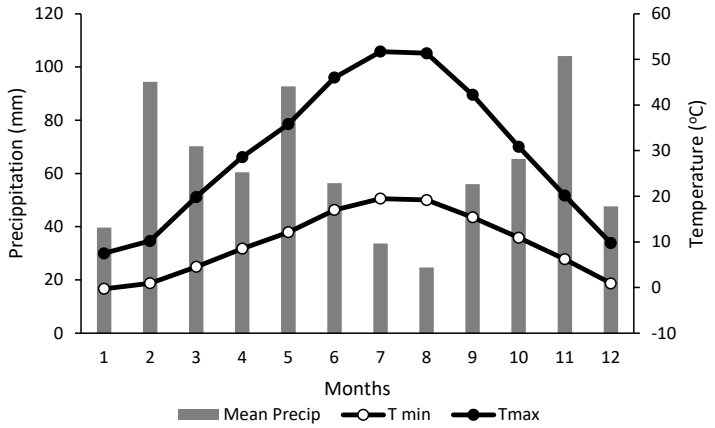

Figure 4.3. Long-term (2011-2020) climatic characterization of the Chiarini 2 experimental in Bologna, Italy.

5. YNCREA, FRANCE

5.1. Site presentation

Located between the 'Nord' and the 'Pas-de-Calais' counties in the former French coal basin, the contaminated area of "Metaleurop Nord" covers an area of 120 km^2 affected by the past metallurgical activities of a lead and zinc smelter: Metaleurop Nord in Noyelle-Godault, France (Figure 5.1). The smelter closed in 2003 but one century of atmospheric dust emissions generated by the plant's chimneys durably contaminated the upper soil layers mostly in Cd, Pb and Zn. The contaminated area includes 10 municipalities and encompasses various land uses: agricultural, urban, industrial, forests, parks etc.

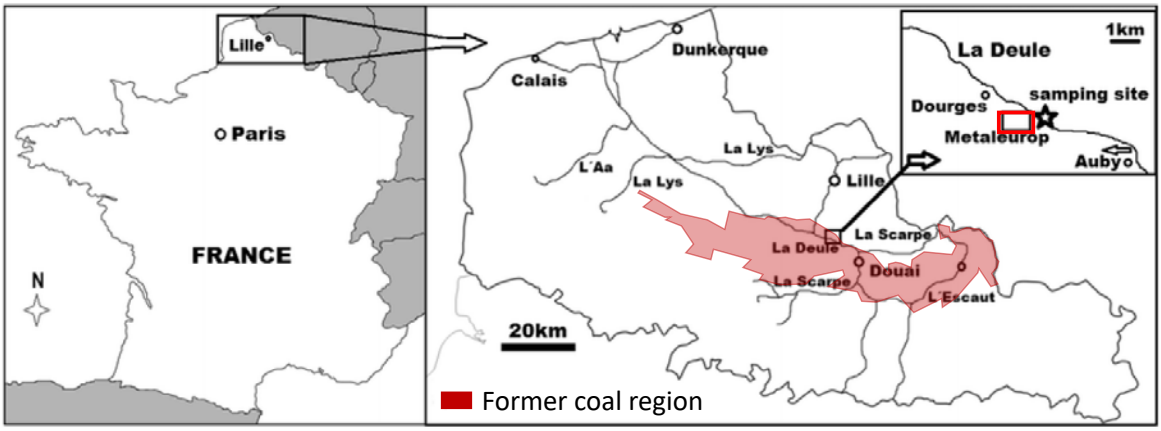

Figure 5.1. Map of Metaleurop site in the former coal region.

The agricultural activities are particularly affected in this area with mean total soil Cd, Pb and Zn respectively 13, 9 and 6 times higher than the regional agricultural background values (Douay, et al., 2007). Thus, since 2015, the health provisions have been reinforced by two prefectural decrees that restrict the sale of agricultural products of animal and plant origin (in compliance with the EU Directive regarding Pb and Cd in crops and food) (Douay, et al., 2012). Restricted perimeters have been defined based on the Cd and/or Pb concentrations of agricultural topsoils and established based on a risk assessment (Pelfrêne et al., 2011). Thus, there is the need to reorient the local agricultural production towards the non-food sector.

In the frame of the Gold project, one experimental plot of 0.35 ha contaminated by Cd, Pb, Zn and Cu and located in Evin-Malmaison (Figure 5.2) was selected by the French partners, i.e. Junia and INRAE, (GPS Coordinates: 50°26'17.3"N 3°01'05.8"E) to grow non-food crops. This plot is located, approximately 700 m further north of the former smelter. It was previously used as an agricultural field where crops such as wheat and sugar beets were cultivated. Nowadays, the site presents a flat ploughed area covered by herbaceous plant species. Before the characterization of the plot, no data were available for this plot, but the surroundings are listed in the French SAFIR network and are extensively studied.

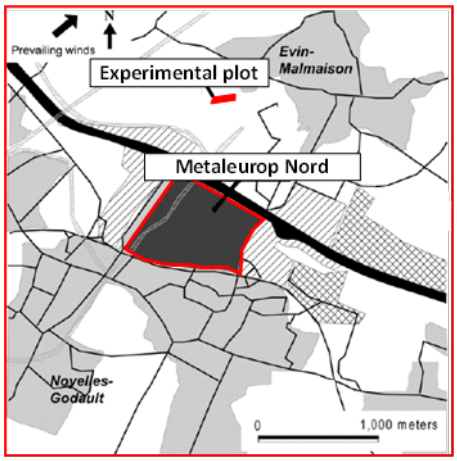

Figure 5.2. Experimental plot in Evin-Malmaison (Google Earth, 2022).

5.2. Soil physico-chemical properties and contamination

Before the soil sampling campaign, a grid covering the whole site was created with a distance between each sampling points of 10 meters. Each sampling point position was located with GPS-related coordinates. Topsoil samples (0-25cm) were taken on the 26th of October 2021 by the 2 French partners (i.e. YNCREA and INRAE), using augers (Figure 5.3). Four subsamples were taken within a zone of around 0.5 m diameter around each sampling point and then mixed to form a more representative composite sample. The sampled residue was then stored in plastic container at room temperature before further analyses. In total, 50 samples were taken on the experimental plot, as shown in Figure 5.3.

Figure 5.3. Scheme and photo of the sampling campaign.

The soil of the plot has developed on colluvial deposits located on the northern edge of the Deûle canal (Aligon et al. 2011). Its pedogenic development links it to redoxic COLLUVIOSOLS. It is a fine silt soil composed of 56% silt, 26% sand, and 18% clay (Table 5.1).

The mean pH value was 7.9 ± 0.2, which characterized the soil as slightly alkaline. The electrical conductivity mean was 122.18 ± 17.11 µS cm^{-1}. The soil from the experimental plot presented in overall good agronomic properties. The cation exchange capacity (CEC) of 13.6 ± 0.8 $cmol^{+}$ kg^{-1}, indicated a good reserve for exchangeable cations, sufficient to meet the nutritional needs of plants and to limit the mobility of metallic cations in excess (i.e. Cd^{2+}, $Cu^{2+,}$ Pb^{2+} and Zn^{2+}) due to anthropogenic activities. With an assimilable phosphorus content of 0.11‰, the soil of the experimental plot was considered moderately rich in this element, which bears witness to a reasonable use of inorganic fertilizer in this agricultural field. Also, the concentrations of both soil

exchangeable cations and assimilable phosphorus were in the same range than those of the regional uncontaminated agricultural soils.

The soil was well supplied with organic matter (36.4 ± 6.9 g kg^{-1}). If the organic carbon concentrations were almost similar to those measured in uncontaminated agricultural soils, this trend was not true for total nitrogen, which was lower on the soil of the experimental plot (i.e. 1.3 ± 0.2 g kg^{-1}) compared to the control soil (i.e. 9.2 g kg^{-1}) resulting in a high C/N ratio of around 16. This result suggested a slowdown in the mineralization of organic matter explained by a reduced soil biological activity linked to soil pollution, already shown is the Metaleurop Safir platform (Pruvot et al., 2002; Aligon et al. 2011). Also, reaction (e.g. encapsulation) of organic matter with carbonates may also contribute to stabilize this organic carbon.

The metal concentrations in the soil varied from 18.7 to 33.5 mg Cu kg^{-1}, 5.7 to 13.8 mg Cd kg^{-1}, 303 to 645 mg Pb kg^{-1}, and 530 to 1411 mg Zn kg^{-1}, showing a soil contamination in Cd, Pb and Zn compared to the pedogeological background in the North of France (i.e. 14.9 mg Cu kg^{-1}, 0.4 mg Cd kg^{-1}, 32.5 mg Pb kg^{-1} and 68.5 mg Zn kg^{-1}, Sterckeman et al., 2002) .The $Ca(NO_3)_2$- extraction showed that Cd and Cu were the highest exchangeable metals (i.e. 6.5 and 6.6 % respectively) and Pb and Zn the least exchangeable metals (i.e. 1.0 and 0.4 %, respectively) compared to the total soil concentrations.

Table 5.1. Physico-chemical properties of the soil from the experimental plot compared with those of an unpolluted regional agricultural soil. Values marked in red are above the pedogeological background in the North of France (Sterckeman et al., 2002).

Parameters	Units	New plot	Uncontaminated agricultural soil [1]
Clay	g kg^{-1}	180.63 ± 8.83	180
Fine silt		191.63 ± 10.24	245
Coarse silt		364.75 ± 7.09	447
Fine sand		224.25 ± 11.30	93
Coarse sand		39 ± 2.88	35
pH		7.91 ± 0.21	6.8
EC	µS cm^{-1}	122.18 ± 17.11	-
CEC Metson	$cmol^{+}$ kg^{-1}	13.6 ± 0.8	-
Organic Carbon	g kg^{-1}	21.02 ± 3.97	18.6
Organic matter	g kg^{-1}	36.38 ± 6.86	-
Total Carbonates	g kg^{-1}	4.18 ± 4.25	4
Total Nitrogen	g kg^{-1}	1.32 ± 0.18	2.02
C/N		15.88 ± 0.88	9.2
Exchangeable K_2O	g kg^{-1}	0.36 ± 0.08	0.19
Exchangeable MgO		0.14 ± 0.02	0.21
Exchangeable CaO		5.63 ± 0.95	4.04
Exchangeable Na_2O		0.02 ± 0.01	0.03
Extractable P_2O_5 (Olsen)		0.11 ± 0.03	0.22
Total Cu	mg kg^{-1}	25 ± 3	14,9
Extractable Cu		1.65 ± 0.77	-
Total Cd		11 ± 2	0.39
Extractable Cd		0.71 ± 0.16	-
Total Pb		536 ± 70	31
Extractable Pb		5.13 ± 1.84	-
Total Zn		955 ± 151	71
Extractable Zn		4.02 ± 3.22	-

[1] *Aligon et al. 2011*

Overall, the contamination was quite heterogeneous on the plot for the four elements (Figure 5.4). A slight contamination gradient was observed depending on the distance to the border of the plot. The spots with the highest concentrations in Cd, Pb and Zn correspond to the locations where the soil is never tilled. In the center of the plot, the contamination deposited in the first centimeter of the plot was tilled and diluted through time in a bigger soil layer as shown by Aligon et al. (2011). This trend will be considered during the creation of the future plots. Additional data on $Ca(NO_3)_2$- extractable Cu, Cd, Pb and Zn are still waited and will allow us to create news maps for extractable concentrations.
The concentrations of the other elements in the topsoil being in the range of the frequent values in most of the study from the Metaleurop Safir platform (Douay, 2014), the rest of this study focuses on Cd, Cu, Pb and Zn.

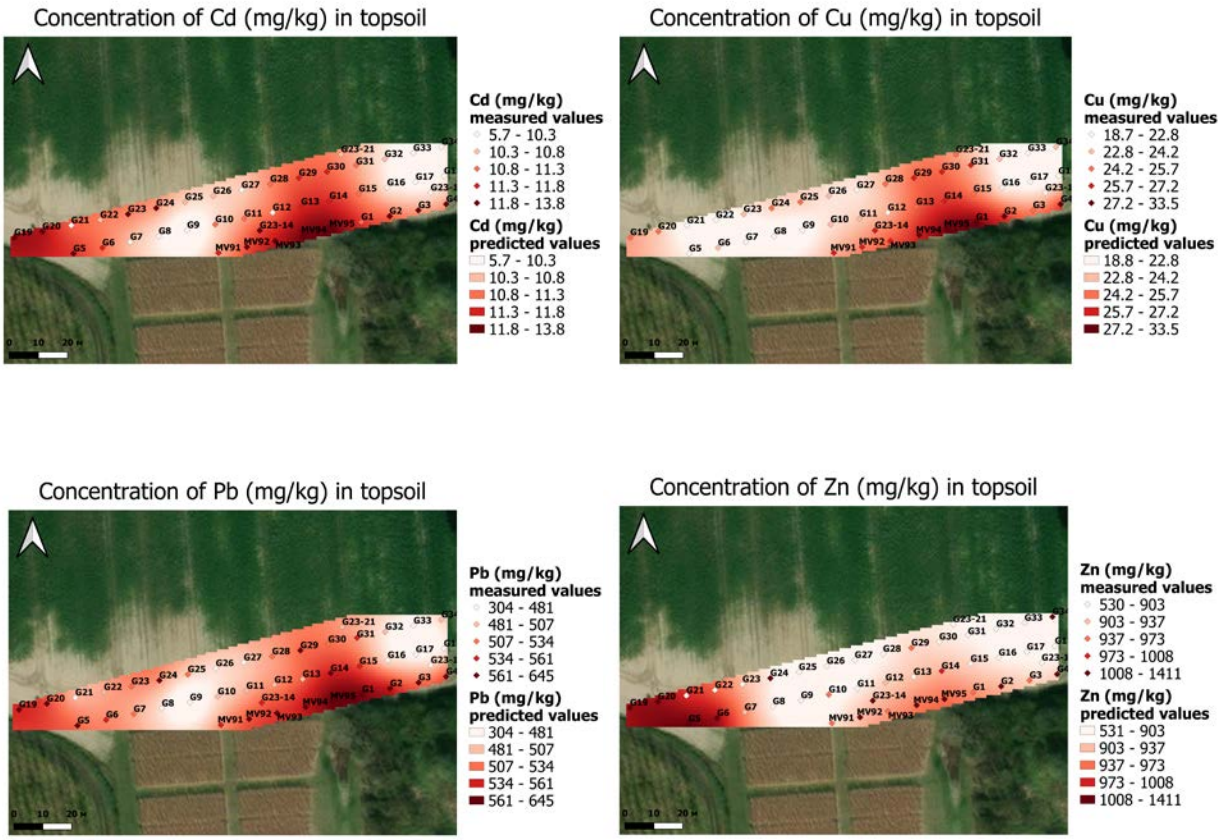

Figure 5.4. Map of soil Cu, Cd, Pb and Zn concentration (mg kg^{-1}) in topsoil (0-25 cm) in the experimental plot.

5.3. Climatic data

The data is taken from the Lesquin meteorological station located 15 kilometres away from the experimental plot.

The region benefits from a temperate climate of oceanic type with a continental trend. The average annual temperature measured over the last 5 years was 12°C. It rarely go below -5°C. The region was exposed to cold winter in 1982, 1985 and 1997 with value ranging between -10 and -20°C for more than 8 days.

The sum of precipitation values (in mm) from 2016 to 2020 is shown in Figure 5.5.A. In 2016, the precipitations were unusually abundant during the months of May and June, with a sum of precipitation over the year reaching 836 mm per year. In 2017, April month was drier than usual and the sum of precipitation over the year was 556 mm per year. Except for these two years, the sum of precipitation for 2018, 2019 and 2020 was around 670 mm per year, with a quite constant values of precipitations through the year around 55 mm per month.

The distribution of min and max temperature values per month for the five studied years were not spread showing a quite stable temperature values over these five years (Figure 5.5.B). The warmer months were July and August with a mean min and max temperature per month of 14 and 25°C, respectively. The coldest months were December and January with a mean min and max temperature per month of 2 and 7°C, respectively.

Ombrothermal diagram describe the climate in the region, by comparing the sum of precipitations and the average temperature in a month, dry or humid months can be highlighted (Figure 5.5.C). In 2020, the sum of precipitation for May and July 2020 were below the min and max temperature curve, indicating that both months were dry. On the opposite, the sum of precipitations was above the temperature curve for the other months, which describes them as humid and rainy.

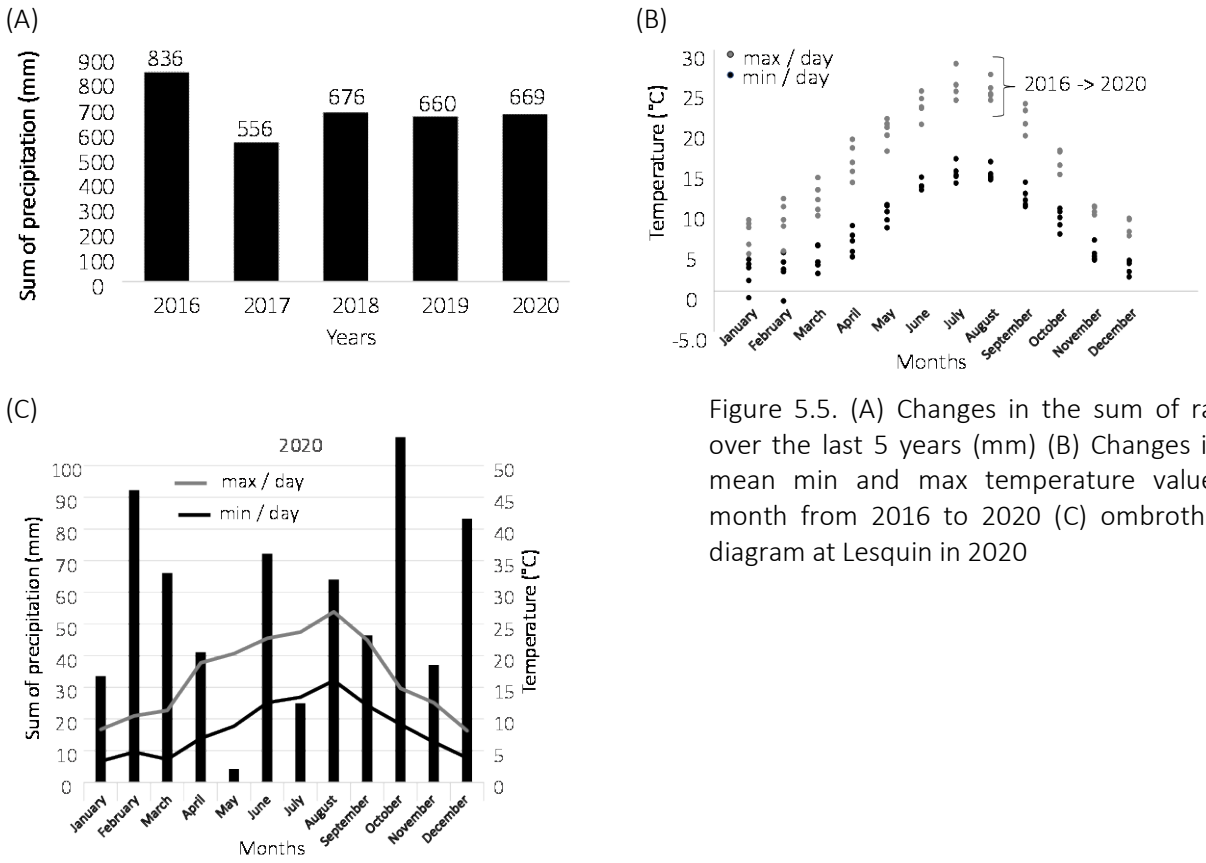

Figure 5.5. (A) Changes in the sum of rainfall over the last 5 years (mm) (B) Changes in the mean min and max temperature value per month from 2016 to 2020 (C) ombrothermal diagram at Lesquin in 2020

Changes in average relative humidity over time are presented in Figure 5.6. Through the last 5 years, the average relative humidity didn't evolve much during winter and autumn but during spring and summer a gap is increasing with a difference of average relative humidity of 15 % between 2016 and 2020 (Figure 5.6.A). The average humidity (in %) slightly evolves over the year 2020, January and December being the most humid months with a relative humidity reaching 89.4% and 90.6%, respectively. April and May were the driest months with an average relative humidity reaching 59.9% and 57.7%, respectively (Figure 5.6.B).

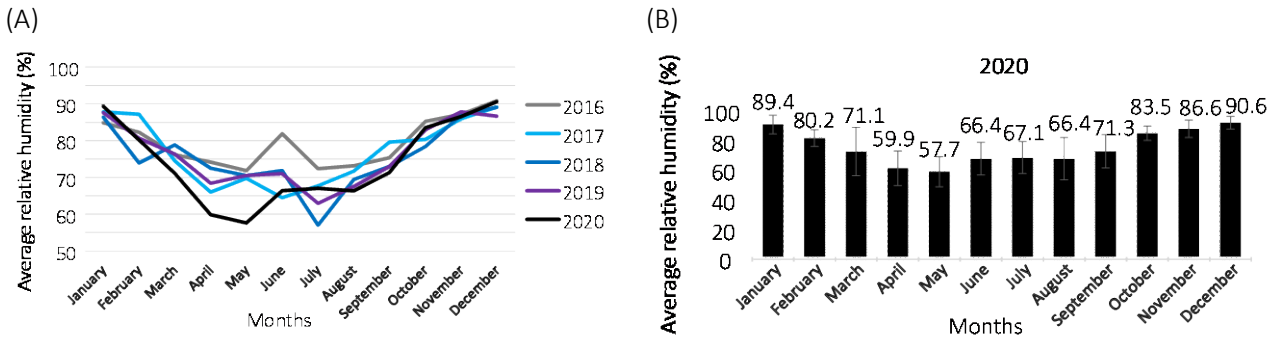

Figure 5.6. Average relative humidity (%) at Lesquin. (A) variation trend through 5 years and (B) variation trend through a year (in 2020).

The prevailing winds are from the southwest sector (Figure 5.7.A) with a speed ranging from 2-4 m s^{-1} to > 8 m s^{-1}. The max wind speed per month is shown in Figure 5.7.B. The year 2016 had the months with the highest max wind speed, with a value for January which reached 107.4 km h^{-1} while 2018 was the year with the lowest max wind speed values. Except for 2016, max wind speed in 2017; 2018, 2019, and 2020 were included in the 40 - 60 km h^{-1} range.

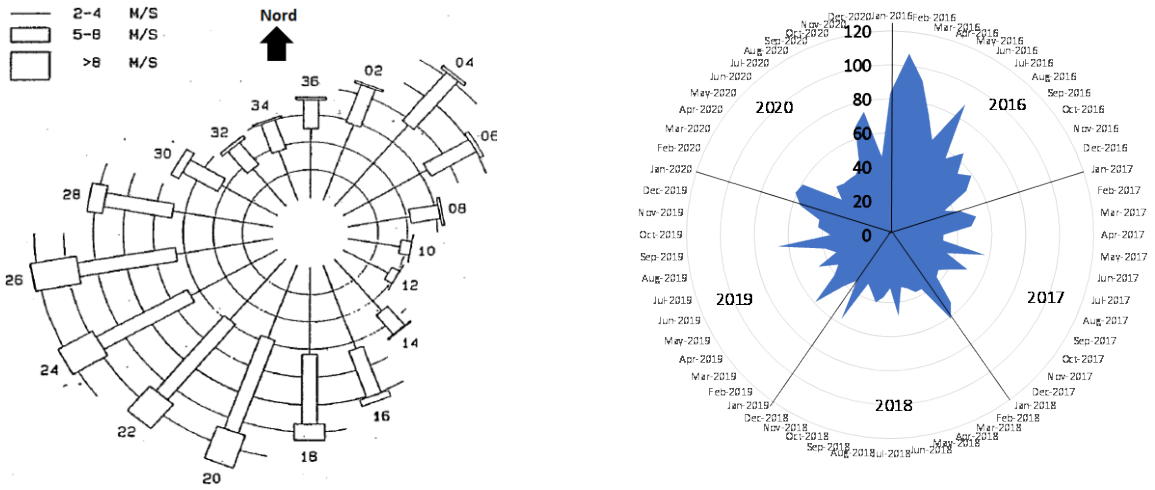

Figure 5.7. (A) Frequencies of mean wind directions (in %), by speed (2-4, 5-8 and >8 m s^{-1}) (Aligon et al. 2011) and (B) mean max wind velocity through 5 years (in km h^{-1})

6. IBFC, CHINA

6.1. Site presentation

Hunan Province is located in Central China and a large area of its farmland is contaminated with heavy metals due to mining activities, sewage irrigation etc (Cao et al., 2020; Su et al., 2021). Among the heavy metals, cadmium has attracted more attention due to its high toxicity, strong mobility, and easy bioconcentration in the food chain (Zhao et al., 2021a). The experimental field chosen for the field experiment is located in Yonghe

Town, Liuyang, Changsha, Hunan, China (28°16′42"N, 113°55′21"E, Figure 6.1). This region belongs to subtropical monsoon climate. The soil has a sandy clay texture and is classified as paddy soil.

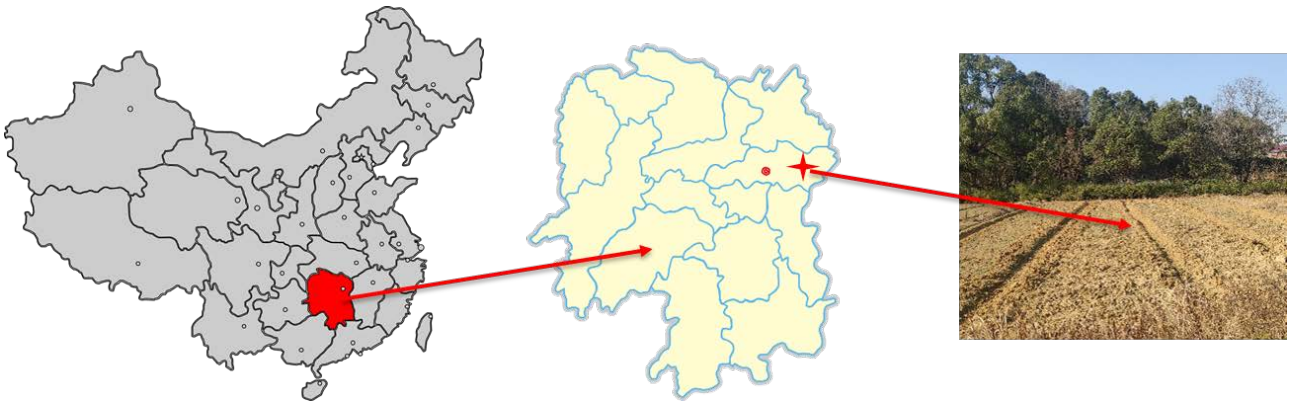

Figure 6.1. Map of field trial site in Hunan, China.

6.2. Soil physico-chemical properties and contamination.

Five soil samples were collected using a sampler at a soil depth of 0.2 m. The results from soil analyses are presented in Table 6.1.

Table 6.1. Basic physicochemical properties of the soil collected from the experimental field.

Sand	Silt	Clay	Organic matter	Total N	Available P	Available K	EC	Soil pH
%			g kg^{-1}	mg kg^{-1}			µS cm^{-1}	
55.5	21.1	23.4	25.8	780	1.4	93	206	4.83

The selected field is located in the typical heavy metal-contaminated area and is close to a large digging. The total cadmium and lead is presented in Table 6.2.

Table 6.2: Heavy metal concentration of the soil collected from the experimental field. Values in red are above the threshold values reported by Duzgoren-Aydin et al., 2006; Chen et al., 2018; Su et al., 2022.

Selected heavy metal	Total concentration (mg kg^{-1})	Threshold values (mg kg^{-1})
Cadmium	1.96 ± 0.20	0.3
Lead	169 ± 10.0	250-350

bdl: below detection limit

6.3. Climatic data.

The monthly average temperature, maximum temperature, and minimum temperature (Figure 6.2) were calculated based on the data (2017-2021) collected from the meteorological station. The highest temperature occurred between July and August. The average temperatures were above 20℃ from May to September.

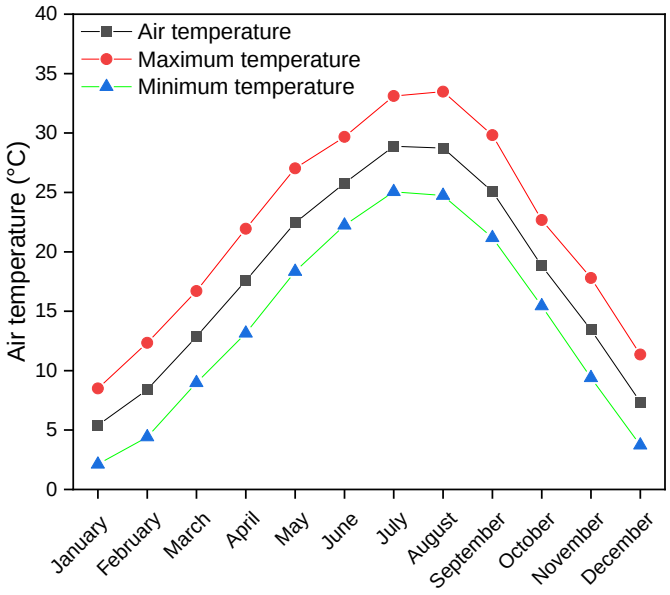

Figure 6.2. Monthly mean, maximum, and minimum air temperature from 2017 to 2021.

Wet precipitation can supply both water and nutrient for crops and is also an important factor affecting crop growth and yield. Over the five years, the annual wet precipitation was more than 1500 mm (Figure 6.3A). The highest wet precipitation happened in June followed by May and July. The average wet precipitations were above 100 mm from March to August. The monthly average relative humidity was also calculated. Over the five years, the relative humidity varied from 71.8% to 80.9%, with the lowest and highest value in December and June, respectively.

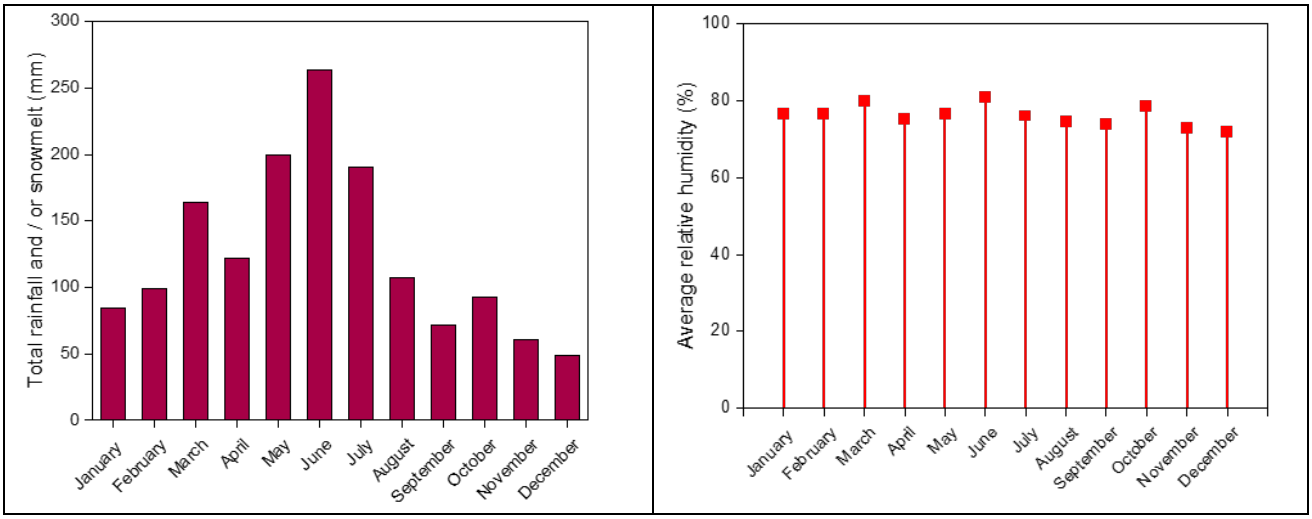

Figure 6.3. Monthly average precipitation and average relative humidity from 2017 to 2021.

The monthly average wind speed varied from 8.24 to 10.6 km/h with the lowest and highest wind speed in June and February (Figure 6.4).

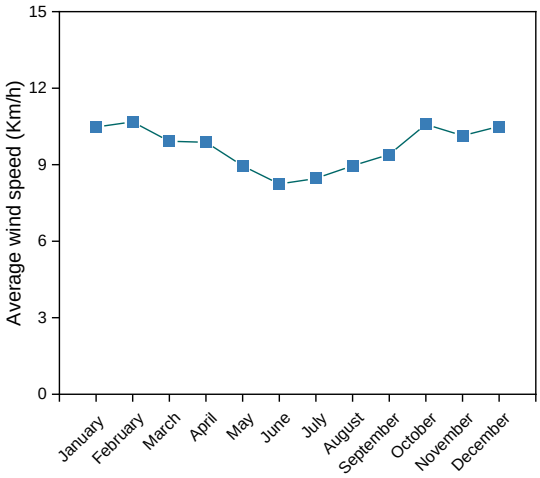

Figure 6.4. Monthly average wind speed from 2016 to 2020.

7. HUNAU, CHINA

7.1. Site presentation

Hunan, a province in South China is known for rice production, contributing about 15% of the total national rice production (Wang et al., 2019). In recent times due to rising cadmium contamination, rice production had been affected drastically. Thus, local government is carrying out different projects and formulate strategies to overcome the challenge of cadmium contamination. The soil of this area is red clay with subtropical monsoon climate. The location of the planned field trials is presented through following map in Figure 7.1.

Figure 7.1. Map of field trial site in Hunan, China (Google Maps, 2022).

There are 3 major reasons for soil contamination in this area: 1) long term use of sewage water for irrigation purposes; 2) atmospheric dust deposition; 3) use of mining water for irrigation. Due to rapid industrialization, large amount of pollutants are being released and these pollutants are managed poorly which is contaminating soil as well as water and entering into food chain. These contaminants enter to water bodies, which subsequently is being used for irrigation purposes in rice production (Huang et al., 2019). It has been reported that approximately 50 million tonnes of mine waste per year is being produced and it is directly contaminating the nearby river.

The selected site is located in Paishangcun village, Lukou District along the Xiang river in Zhuzhou, Hunan, China (27.72708 N, 113.180581 E). The total area of the Lokou district is 1053.62 Km^2. Since long, it has been the main mining area, which is why overall the heavy metal contents in soil is high.

7.2. Soil physico-chemical properties and contamination

Four composite soil samples were collected from the experimental site by using soil augur. In Table 7.1 soil macronutrients (NPK) along with organic matter, soil pH and soil conductivity are presented. Soil texture is presented in Figure 7.2.

Table 7.1. Basic soil physical and chemical properties.

Soil parameters					
Organic matter (g kg^{-1})	N (g kg^{-1})	P (g kg^{-1})	K (g kg^{-1})	EC (uS cm^{-1})	Soil pH
0.0084 ± 0.001	1.1820 ± 0.21	0.0171 ± 0.002	0.4060 ± 0.03	128.87 ± 12.35	6.1 ± 0.32

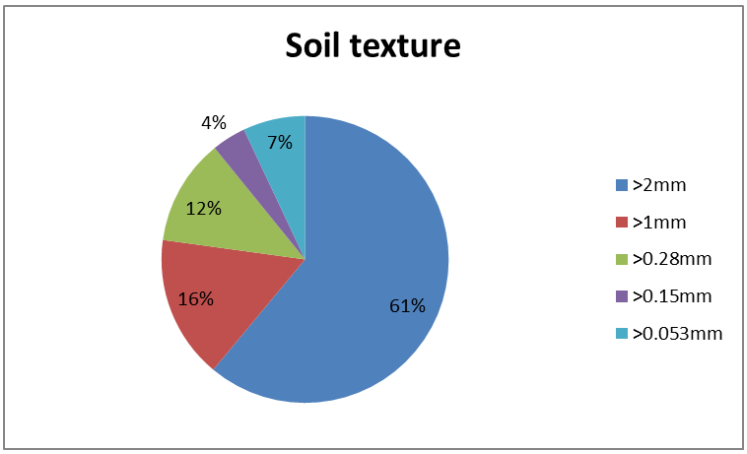

Figure 7.2. Share of specific ranges of particle sizes.

As this area is one of the mining areas and soil is contaminated with heavy metals, therefore soil samples were collected and analysed for selected heavy metal contents. The total cadmium, chromium and lead is presented in the following Table 7.2.

Table 7.2. Heavy metal content in the collected samples. Values in red are above the threshold values reported by Duzgoren-Aydin et al., 2006; Chen et al., 2018; Su et al., 2022.

Heavy metals	Total concentrations (mg kg^{-1})	Threshold values (mg kg^{-1})
Cadmium	3.75 ± 0.23	0.3
Chromium	123.75 ± 9.13	200
Lead	217.25 ± 19.27	250-350

.

7.3. Climatic data.

Climate data is comprised of long term data of precipitation, temperature, relative humidity and wind speed.

Mean precipitation, minimum and maximum temperature for each month (2016-2020) was calculated and presented in Figure 7.3.A. In each year, more than 40% of total precipitation took place in three months (May to July) except for 2018 where it was 32%. Overall, the highest total precipitation was recorded during 2016

followed by 2020, whereas lowest was recorded in 2017. The sum of precipitation for each year is presented in the Figure 7.3.B.

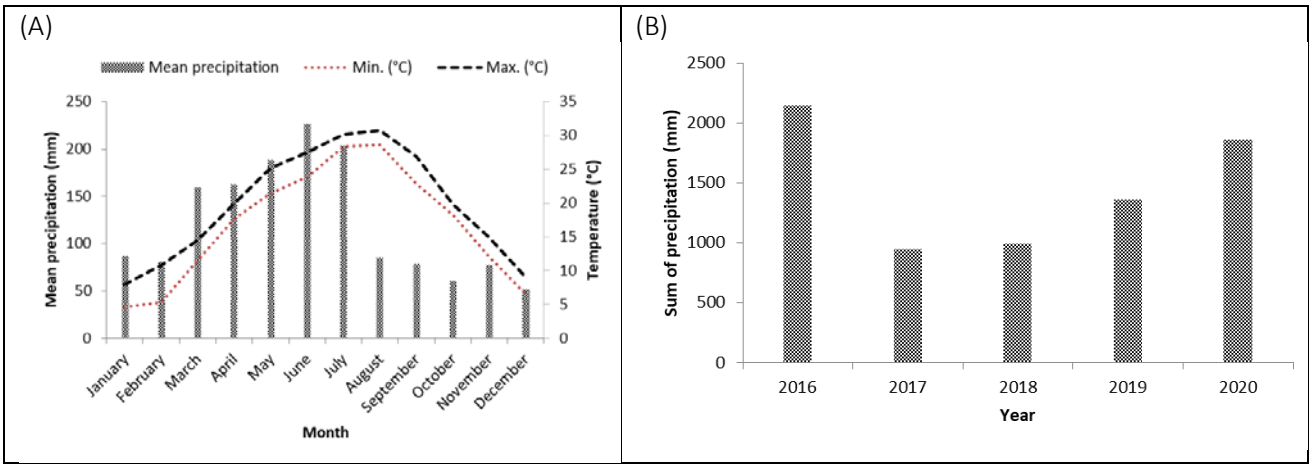

Figure 7.3. (A) Mean, minimum and maximum precipitation per month, along with temperature (B) Sum of precipitation from 2016 to 2020.

Over the years, mean temperature did not fluctuate significantly. Each year, January was recorded as the coldest month (Figure 7.4.A), whereas highest temperature was recorded during July-August. In January, the temperature varied from 4.6 to 8 °C, whereas in hottest months of the year (July-August), temperature varied from 28 to 31 °C. The relative humidity varied from 70% to 83% (Figure 7.4.B).

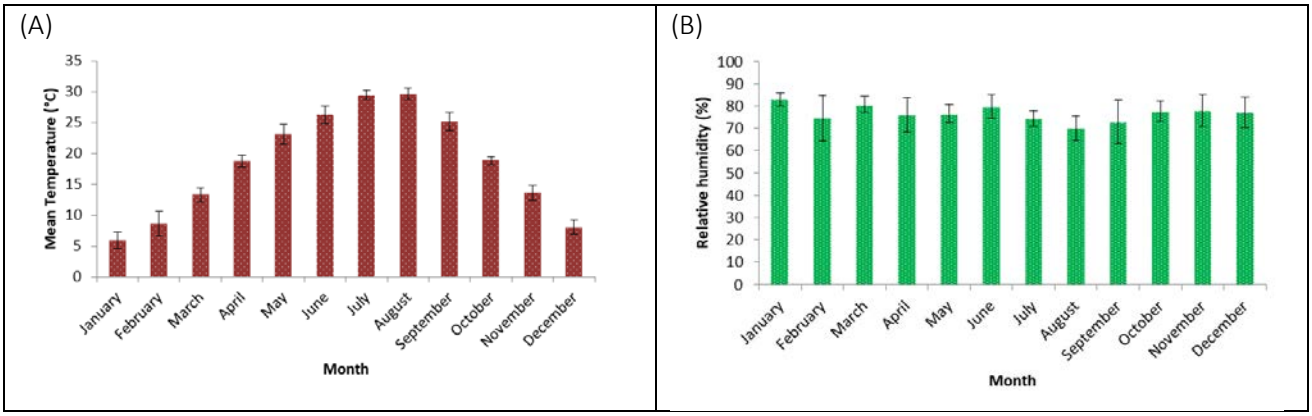

Figure 7.4. Mean temperature and relative humidity from 2016 to 2020 for each month. Error bars indicate the standard deviation

The wind speed is presented in Figure 7.5. Over the years the lowest wind speed was recorded during July , whereas highest was recorded in October followed by January-February.

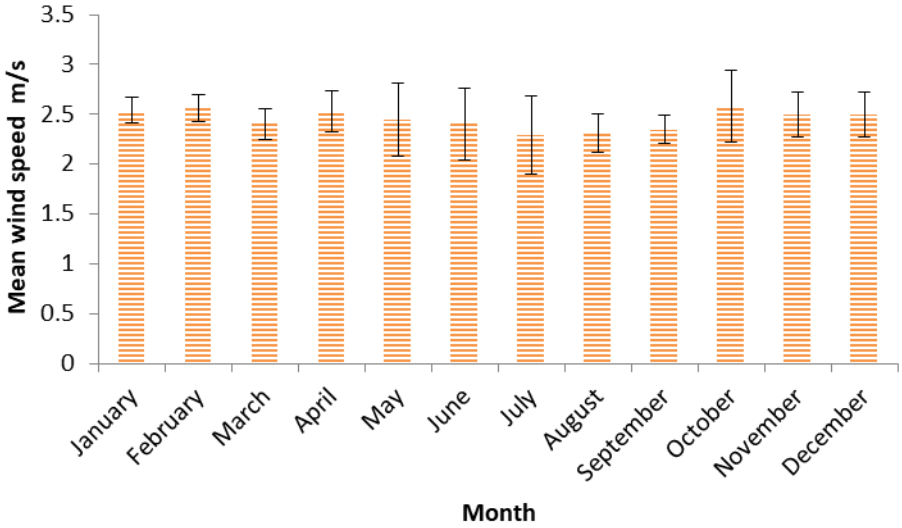

Figure 7.5. Mean wind speed over the years (2016-2020) for each year. Error bars indicate standard deviation.

CONCLUSSIONS

The Gold partner countries and experimental fields cover a wide range of agro-ecological climatic zones. The experimental fields are arable land contaminated with different species of heavy metals and metalloids at various levels. The most frequently found element is Cd, determined in the fields of AUA, UMCS, YNCREA, IBFC, HUNAU. Next are the elements: Pb and Zn (AUA, UMCS, UNIBO, YNCREA); Ni (AUA, CRES, UNIBO); AS (AUA, CRES, UMCS); Cu (UNIBO, YNCREA). In one site the elements Cr (CRES), Sn (UNIBO), Co (CRES), Sb (AUA) are found. These sites poses risks for human health if they are used for food production or grazing and are in need for remediation. Therefore, developing, presenting and promoting the GOLD green technology is an important step of improvement, and will be a valuable guide to mitigate the exposure route for the intake of contaminants by humans.

References

Aligon, D., Douay, F. 2011. Site atelier Metaleurop: Synthèse des travaux de recherche réalises autour de l'ancienne fonderie de Noyelles-Godault. Rapport de synthèse ADEME.

Cao, X., Tan, C., Wu, L., Luo, Y., He, Q., Liang, Y., Peng, B., Christie, P. 2020. Atmospheric deposition of cadmium in an urbanized region and the effect of simulated wet precipitation on the uptake performance of rice. The Science of the Total Environment 700, 134513. doi: 10.1016/j.scitotenv.2019.134513.

Douay, F., Pruvot, C., Roussel, H., Fourrier, H., Ciesielski, H., Proix, N., Waterlot, C. 2007. Contamination of urban soils in an area of northern France polluted by dust emissions of two smelters. Water Air and Soil Pollution 188, 247-260. doi: 10.1007/s11270-007-9541-7.

Douay, F., Pelfrêne, A., Planque, J., Fourrier, H., Richard, A., Roussel, H., Girondelot, B. 2012. Assessment of potential health risk for inhabitants living near a former lead smelter. Part 1: metal concentrations in soils, agricultural crops, and homegrown vegetables. Environmental Monitoring and Assessment 185, 3665-3680. doi: 10.1007/s10661-012-2818-3.

Douay, F. 2014. Développement de la phytostabilisation sur des sols contaminés par des métaux à des fins énergétiques : viabilité écologique, intérêt social et bilan économique. Groupe ISA, Equipe Sols et Environnement, ADEME, Rapport PHYTENER.

Duzgoren-Aydin, N.S., Wong, C., Aydin, A., Song, Z., You, M. and Li, X.D. 2006. Heavy metal contamination and distribution in the urban environment of Guangzhou, SE China. Environmental Geochemistry and Health 28, 375-391.

Huang, Y., Wang, L., Wang, W., Li, T., He, Z., Yang, X. 2019. Current status of agricultural soil pollution by heavy metals in China: A meta-analysis. The Science of the Total Environment 651, 3034–3042. doi: 10.1016/j.scitotenv.2018.10.185.

Kabata-Pendias, 2000. Trace elements in soils and plants. doi: 10.1201/9781420039900.

Kabata-Pendias, A., Mukherjee, A.B., 2007. Trace Elements from Soil to Human. Springer-Verlag, Berlin, Heidelberg.

Kakavoyiannis, E.C. 2005. Μέταλλα εργάσιμα και συγκεχωρημένα: η οργάνωση της εκμετάλλευσης του ορυκτού πλούτου της Λαυρεωτικής από την Αθηναϊκή Δημοκρατία. Archaeological Receipts Fund, Athens. ISBN: 9789602144404.

Kakavoyianni, O., Douni, K., Nezeri, F. 2008. Silver metallurgical finds dating from the end of the final Neolithic period until the middle Bronze Age in the area of the Mesogeia. In: Tzachili, I. (Ed.), Aegean metallurgy in the Bronze Age. Proceedings of International Symposium, University of Crete, Rethymnon, Greece, 45–57.

Kucharski, R., Rostański, A., Sas-Nowosielska, A., Płaza, G., Gucwa-Przepióra, E., Sobik-Szołtysek, J., Krzyżak, J., Wąsowicz, P. 2010. Evaluation of ecological conditions and the current state of vegetation cover of two waste heaps "Dołki" in Piekary Śląskie (Poland) as a basis for planning land rehabilitation process and further development. In: Skowronek, J. (Ed.), Innowacyjne rozwiązania rewitalizacji terenów zdegradowanych 2010 (*in Polish*). Katowice, Wydawnictwo Centrum Badań Górnictwa Podziemnego w Katowicach, Instytut Ekologii Terenów Uprzemysłowionych w Katowicach, pp. 64–73.

Kumpiene, J., Giagnoni, L., Marschner, B., Denys, S., Mench, M., Adriaensen, K., Vangronsveld, J., Puschenreiter, M., Renella, G. 2017. Assessment of Methods for Determining Bioavailability of Trace Elements in Soils: A Review. Pedosphere 27, 389-406. doi: 10.1016/S1002-0160(17)60337-0.

Mench, M.J., Dellise, M., Bes, C.M., Marchand, L., Kolbas, A., Le Coustumer, P., Oustrière, N. 2018. Phytomanagement and remediation of Cu-contaminated soils by high yielding crops at a former wood preservation site: Sunflower biomass and ionome. Frontiers in Ecology and Evolution 6, 123. https://doi.org/10.3389/fevo.2018.00123.

Ministry of Environment, 2002. The regulation of the Ministry of Environment on standards for soil quality and earth quality standards. 9.09.2002. Dz. U. Nr 165, poz. 1359. Ministry of Environment: Warsaw, Poland.

Panagos, P., Van Liedekerke, M., Yigini, Y., Montanarella, L. 2013. Contaminated Sites in Europe: Review of the current situation based on data collected through a European network. Journal of Environmental Public Health, 158764. doi: 10.1155/2013/158764.

Papadopoulos, A., Prochaska, C., Papadopoulos, F., Gantidis, N., Metaxa, E. 2007. Determination and evaluation of cadmium, copper, nickel, and zinc in agricultural soils of Western Macedonia, Greece. Environmental Management 40, 719-726. doi: 10.1007/s00267-007-0073-0.

Paya Perez, A., Rodriguez Eugenio, N. 2018. Status of local soil contamination in Europe: Revision of the indicator "Progress in the management contaminated sites in Europe", EUR 29124 EN, Luxembourg: Publications Office of the European Union. doi:10.2760/093804 JRC107508.

Pelfrëne, A., Waterlot, C., Mazzuca, M., Nisse, C., Bidar, G., Douay, F. 2011. Assessing Cd, Pb, Zn human bioaccessibility in smelter-contaminated agricultural topsoils (northern France). Environmental Geochemistry and Health 33, 477-493. doi: 10.1007/s10653-010-9365-z.

Pruvot, C., Douay, F., Emis, A., Dubourguier, H.C., Schvartz, C. 2002. Etude des conditions de minéralisation de la matière organique dans les sols pollués. Programme de Recherches Concertées. Environnement et Activités humaines. Etude d'un secteur pollué par les métaux, 108.

Sterckemant, T., Douay, F., Proix, N., Fourriez, H., Perdrix, E. 2002. Assessment of the contamination of cultivated soils by eighteen trace elements around smelters in the North of France. Water, Air, and Soil Pollution 135, 173-194. doi: 10.1023/A:1014758811194.

Su, Y., Wen, Y., Yang, W., Zhang, X., Xia, M., Zhou, N., Xiong, Y., Zhou, Z. 2021. The mechanism transformation of ramie biochar's cadmium adsorption by aging. Bioresource Technology 330, 124947. doi: 10.1016/j.biortech.2021.124947.

Tristan, E., Demetriades, A., Ramsey, M.H., Rosenbaum, M.S., Thornton, I., Vassiliades, E., Vergou-Vichou, K., Kazantzis, G. 1999. Spatially resolved hazard and exposure assessments. In: Demetriades, A. (Ed.), Geochemical atlas of the Lavrion urban area for environmental protection and planning. Institute of Geological and Mineral Exploration, Athens, Vol 1.

Van Liedekerke, M., Prokop, G., Rabl-Berger, S., Kibblewhite, M., Louwagie, G. 2014. Progress in the management of contaminated sites in Europe. EUR 26376. Luxembourg: Publications Office of the European Union; 2013. JRC85913.

Wang, C., Zhang, Z., Zhang, J., Tao, F., Chen, Y., Ding, H., 2019. The effect of terrain factors on rice production: A case study in Hunan Province. Journal of Geographical Sciences 29, 287–305. doi: 10.1007/s11442-019-1597-y.

Wójcik, M., Sugier, P., Siebielec, G. 2014. Metal accumulation strategies in plants spontaneously inhabiting Zn-Pb waste deposits. The Science of the Total Environment 487, 313-322. doi: 10.1016/j.scitotenv.2014.04.024.

Xenidis, A., Papassiopi, N., Komnitsas, K. 2003. Carbonate-rich mining tailings in Lavrion: risk assessment and proposed rehabilitation schemes. Advances in Environmental Research 7, 479–494. doi: 10.1016/S1093-0191(02)00017-5.

Zhao, X., Luan, M., Qiu, C., Guo, Y., Long, S., Wang, Y., Qiu, H. 2021a. Analysis of the potential of 165 ramie germplasms to be used for cadmium-contamination remediation. Industrial Crops and Products 171. doi: 10.1016/j.indcrop.2021.113841.